REEL-C 3881B

A.T.I 80261

UNCLASSIFIED

30 261

An Experimental Investigation of the Coanda Effect - and Appendix (Thesis)

(None)

Marwood, Robert M., Jr.
Purdue University, Engineering Experiment Station, Lafayette, Ind. (None)
(Same)

Feb '49 **Unclass.** **U.S.** **English** **39** **photos, diagrs, graphs** (None)

The Coanda effect is a fluid-flow phenomenon in which fluid constrained to two-dimensional flow and discharged from a rectangular or annular slot will be deflected from its initial direction to flow along the flap. Results are presented of an experimental investigation to determine the entrainment characteristics and efficiencies of a Coanda slot and single flap. It was found that the mechanism of entrainment is equally dependent upon the pressure reduction in the jet and turbulent momentum exchange in the mixing zone. Entrainment can be increased by increasing the overhang at the cost of a reduction in the kinetic energy of the jet. A small overhang and flap angle offers best possibilities for applications in which little reduction in the kinetic energy of the jet is permissible.

Flow, Two-dimensional
Aerodynamics (2) **Slots - Aerodynamic effects**
Fluid Mechanics and Aerodynamic Theory (9)

USAF Contr. No. W33-038-ac-17635

PURDUE UNIVERSITY

ENGINEERING EXPERIMENT STATION

LAFAYETTE, INDIANA

AN EXPERIMENTAL INVESTIGATION

OF

THE COANDA EFFECT

PROJECT NO. M-156

DATE February, 1949

AN EXPERIMENTAL INVESTIGATION

OF

THE COANDA EFFECT

This report is based entirely upon a thesis submitted by Robert M. Marwood, Jr. to the faculty of Purdue University in August, 1948 for the Degree of Master of Science in Mechanical Engineering, and is in partial fulfilment of the Air Force contract #33-038-ac-17625.

Prepared by,

Robert M. Marwood, Jr.

Approved by,

M. J. Zucrow
Prof. of Gas Turbines and
Jet Propulsion

ACKNOWLEDGMENT

The author is deeply grateful to Dr. M. J. Zucrow. His suggestion of the project and his subsequent guidance and inspiration made this investigation possible. The author also sincerely appreciates the invaluable assistence of Dr. C. F. Warner in the direction and preparation of the report. Further thanks are due to Professor J. Liston and Mr. M. O. Dellinger for their aid in securing meterials; to Mr. McCormick, Propulsion Section, Technical Intelligence, Wright Field for securing most of the literature surveyed; and to Mr. C. Yerber and Mr. D. Stough for assistence in calculating and drafting.

ABSTRACT

This report presents the results of an experimental investigation undertaken to determine the entrainment charecteristics and efficiencies of a Coanda slot and single flap. The results obtained indicate that (a) the mechanism of entrainment is equally dependent upon the pressure reduction in the jet and turbulent momentum exchange in the mixing zone; (b) the reduction in kinetic energy along the flap can be attributed to work done by the jet against increasing pressure, losses in the region of separation and losses in the mixing zone between the jet and the surrounding medium; (c) entrainment can be increased by increasing the overhang at the cost of a reduction in the kinetic energy of the jet; and (d) for applications in which little reduction in the kinetic energy of the jet is permissible, a small overhang and flap angle offers the best possibility.

TABLE OF CONTENTS

LIST OF FIGURES

NOTATION

a = overhang

A = area

b = slot height

e = energy ratio = E_x/E_1

E = kinetic energy of fluid passing any section in a time Δt

g = acceleration due to gravity

G = weight rate of flow

h = differential head

k = specific heat ratio

l = Prandtl mixing length

L = length of flap

m = mass-rate ratio = M_x/M_1

M = Mass-rate of flow across any section

p = pressure

q = dynamic pressure = $\rho V^2/2$

r = p/p_T

R = gas constant = 53.3 ft-lb/lb-$^{\circ}$R

R_l = Reynolds number = $\rho_1 V_1 b/\mu_1$

t = time

T = absolute temperature

v = specific volume

V = absolute velocity

w = width of slot

W = compressibility factor to be used in calculating E

x = distance along the flap

Y = compressibility factor to be used in calculating V

Z = compressibility factor to be used in calculating V

Greek

α = flap angle

β = acute angle between the velocity vector and a line perpendicular to the flap

γ = specific weight of fluid

$\eta = \Delta p_1/q_1$ = efficiency of Coanda effect as a pressure reducing device

θ = angle measured by direction finding tube

λ = recovery factor for temperature = $T_i - T / T_T - T$

μ = coefficient of viscosity

ρ = density

τ = turbulent shear stress

ϕ = angle between velocity vector and a line parallel to the flap

Subscripts

1 = at a section in the slot

2 = surrounding medium

a = inches of air

i = indicated

L = left

m = inches of water

R = right

T = total

x = at a section at x distance along the flap from the corner

AN EXPERIMENTAL INVESTIGATION OF THE COANDA EFFECT

INTRODUCTION

A host of ingenious inventions has resulted from the discovery of a fluid-flow phenomenon called the Coanda effect after its discoverer M. Henri Coanda, a Roumanian engineer whose first patent dealing with the application of the effect was filed prior to 1935. The Coanda effect may best be understood by reference to Figure 1, as follows. Fluid constrained to two dimensional flow and discharged from a rectangular or annular slot will be deflected from its initial direction to flow along the flap. This deflection will result in (a) a pressure reduction in the slot and throughout the interior of the jet, (b) an acceleration of the flow in the region of the corner, and (c) an entrainment of fluid from the surrounding medium by the jet. Further deflection of the stream may be accomplished by the addition of a series of such flaps, the preceding phenomenon being repeated at each corner.

The present report is the result of an experimental investigation to determine the entrainment characteristics and efficiencies of a [illegible] slot and single flap. The work has been directed by Dr. M. J. Zucrow and conducted as a thesis in the Department of Mechanical Engineering, Purdue University. The results obtained indicate that (a) the mechanism of entrainment is equally dependent upon the pressure reduction in the jet and turbulent-momentum exchange in the mixing zone; (b) reductions in kinetic energy along the flap are due mainly

to work done by the jet against increasing pressure and to losses in the region of separation; (c) the entrainment may be increased by increasing the overhang at the cost of a reduction in the kinetic energy of the jet; and (d) for applications in which the attainment of high efficiencies is of prime importance, a small overhang and flap angle offers the best possibility.

The report has been presented in three sections: (a) a description of the basic phenomenon, (b) a literature survey, and (c) a description of the experimental work and a discussion of results and conclusions derived therefrom.

DESCRIPTION OF BASIC PHENOMENON

The Coanda effect may best be described by reference to Figure 1, as follows. Fluid constrained to two dimensional flow and discharged from a rectangular or annular slot will be deflected from its initial direction to flow along the flap. This deflection will result in (a) a pressure reduction in the slot and throughout the interior of the jet, (b) an acceleration of the flow in the region of the corner, and (c) an entrainment of fluid from the surrounding medium by the jet. The mechanism of this entrainment can be attributed partly to turbulent momentum exchange between the jet and the surrounding medium and partly to the existence of the region of low pressure. Coanda stated (1)* that the flow may be further deflected up to 180 degrees by the addition of a series of flaps. Optimum angles of divergence quoted by Coanda were 31 degrees for the first flap, 28 degrees for the second and so forth, the angle reducing by approximately three degrees for each additional flap. Work by Boyer (2), however, has indicated that no such optimum angles could be determined without specifying the so-called overhang. This quantity is indicated in the sketch in Figure 1.

The existence of the phenomenon can best be attributed, as shown in Figure 3, to the formation of a starting vortex between the jet and the flap. Considering the jet in the undeflected position, it can be seen that entrainment of the surrounding medium by the jet due to turbulent momentum exchange will result in a reversed flow up the flap.

* Numbers in parentheses refer to bibliography.

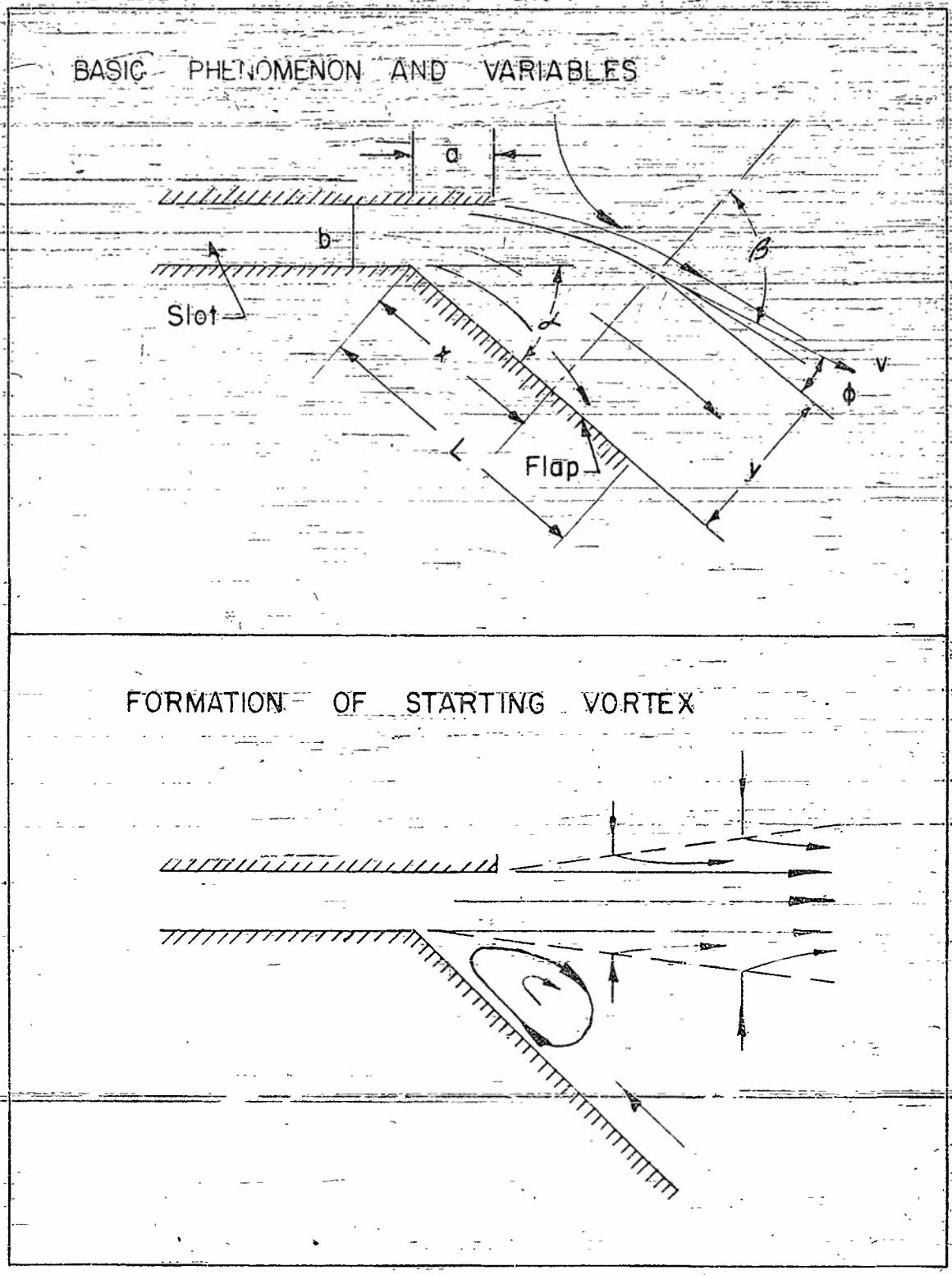
BASIC PHENOMENON AND VARIABLES
a
b
Slot
x
L
Flap
y
V
ϕ
β
α
FORMATION OF STARTING VORTEX

FIG. 1

The starting vortex will then develop as shown in the figure, resulting in a region of low pressure on the under side of the jet. This region of low pressure below the undeflected jet has been noticed by the author in his experimental work, and reversed flow up the flap was detected by Boyer by blowing smoke through static pressure holes along the flap.

A force resulting from the differential between the outside pressure on the upper-side of the jet and the reduced pressure on the under side causes the jet to deflect and follow the flap. Deflection of the jet results in a further decrease in pressure at the corner. This is explained by the incompressible flow theory, which dictates the existence of an infinitely low pressure at the corner. Addition of further flaps results in repetition of the above phenomenon at each succeeding corner.

LITERATURE SURVEY

Theoretical and basic experimental investigations of the Coanda effect are distinctly lacking. Metral (1) has contributed the only theoretical work to date. His report, which was presented at the Fifth International Congress for Applied Mechanics in 1938, assumed the existence of the phenomenon and was based on potential theory. Solution of the potential problem was undertaken with a sequence of conformal transformations and was presented in two infinite series. The first series related α , a/b, β , and V_L/V_1. The second series solution related α , L/b, β , and V_L/V_1. A table was included showing the relation between V_L/V_1 and α for a/b equal to zero, and with a flap of infinite length. This theoretical work of Metral indicated that the ratio V_L/V_1 should increase with increasing flap angle. However, velocity profiles obtained by the author and presented in Figure 14 indicate that the converse is true. This deviation between Metral's theory and the author's experimental results is due to the existence of strong turbulent shear stresses within the jet and to thickening of the region of separation. For L/b greater than 2 Metral found that the direction of flow deviated very slightly from that of the flap and that the ratio V_L/V_1 was practically independent of flap length.

Of considerable importance was the proof by Metral that a region of low pressure exists throughout the jet. This proof followed directly from Bernoulli's Theorem and results indicating that the ratio V_L/V_1 was greater than one for all conditions. His paper also presented a valuable discussion of the effects of compressibility, indicating that

the Coanda effect could not exist if the velocity in the slot exceeds that of sound. The paper stated, too, that experimental work by M. Coanda proved that stable flow could exist only if the pressure gradient along the flap were sufficiently low and that this condition was fulfilled for L/b greater than eight.

The work of Metral is of extreme importance in clarifying the theory of the phenomenon. The results obtained are of little quantitative importance because of the dependence of the effect on viscous forces.

The work conducted by Boyer (2) at Purdue University provided the first experimental investigation of the basic phenomenon. His work was conducted with a Coanda slot and single flap 10 inches in length. The slot had a rectangular cross-section one inch in height by two inches in width. Boyer's work consisted of a systematic measurement of the pressure reductions resulting from the flow around the corner as well as a detailed study of the nature of the phenomenon. His work proved that the effect could exist only in two-dimensional flow. Experiments conducted with no overhang showed that the flow became unstable at a flap angle of 41 degrees and finally detached at 46 degrees. There seemed to be a tendency for this flow to detach at a slightly lower flap angle as the velocity of flow increased. This tendency is supported by Hall (3), who reported that the point of separation of a fluid in a two-dimensional diffuser approaches the throat section with increasing Reynolds number. Boyer also showed that the angle at which detachment occurred decreased decidedly with increasing overhangs until at a/b equal to two the condition of unstable flow began at a flap angle of 33 degrees, and finally the flow detached at 36 degrees.

Boyer also studied the importance of flap angle and overhang upon pressure reduction in tests conducted at a constant setting of a gate valve located in the line between his test section and the blowers. He defined the pressure reduction at any one condition as the difference between the static pressure in the slot for that condition and the static pressure at the same point but with a flap angle of 90 degrees.

His results are reproduced in dimensionless form in Figure 2. Of interest is the effect of Reynolds number upon the results obtained at a/b equal to zero. The three curves corresponding to the higher Reynolds numbers show almost identical characteristics indicating independence of $\Delta p_1/q_1$ from Reynolds number for R_1 greater than 140,000. These curves also indicate that the pressure reduction reaches a maximum at a flap angle of 35 degrees. The effect of overhang is also clearly indicated. The maximum pressure reduction for a/b equal to two is approximately 50 per cent larger than the maximum for no overhang, and it occurs at a flap angle of 20 degrees.

Velocity traverses made by Boyer at the slot exit showed a non-rectilinear distribution along the wall opposite the corner. A traverse 3/4 in. down the flap shows a maximum velocity at the edge of the boundary layer 30 per cent greater than the maximum velocity at the slot exit.

Remaining literature is devoted primarily to descriptions of applications of the Coanda effect and to reporting progress made by M. Coanda in the development of these various applications. Interest in the Coanda effect in the United States was first aroused by three such reports. The first report (4) resulted from a conference of

PRESSURE REDUCTION IN SLOT AS A FUNCTION OF FLAP ANGLE AT DIFFERENT REYNOLDS & OVERHANGS (REPRODUCED FROM BOYER, loc. cit.)

L/b = 10

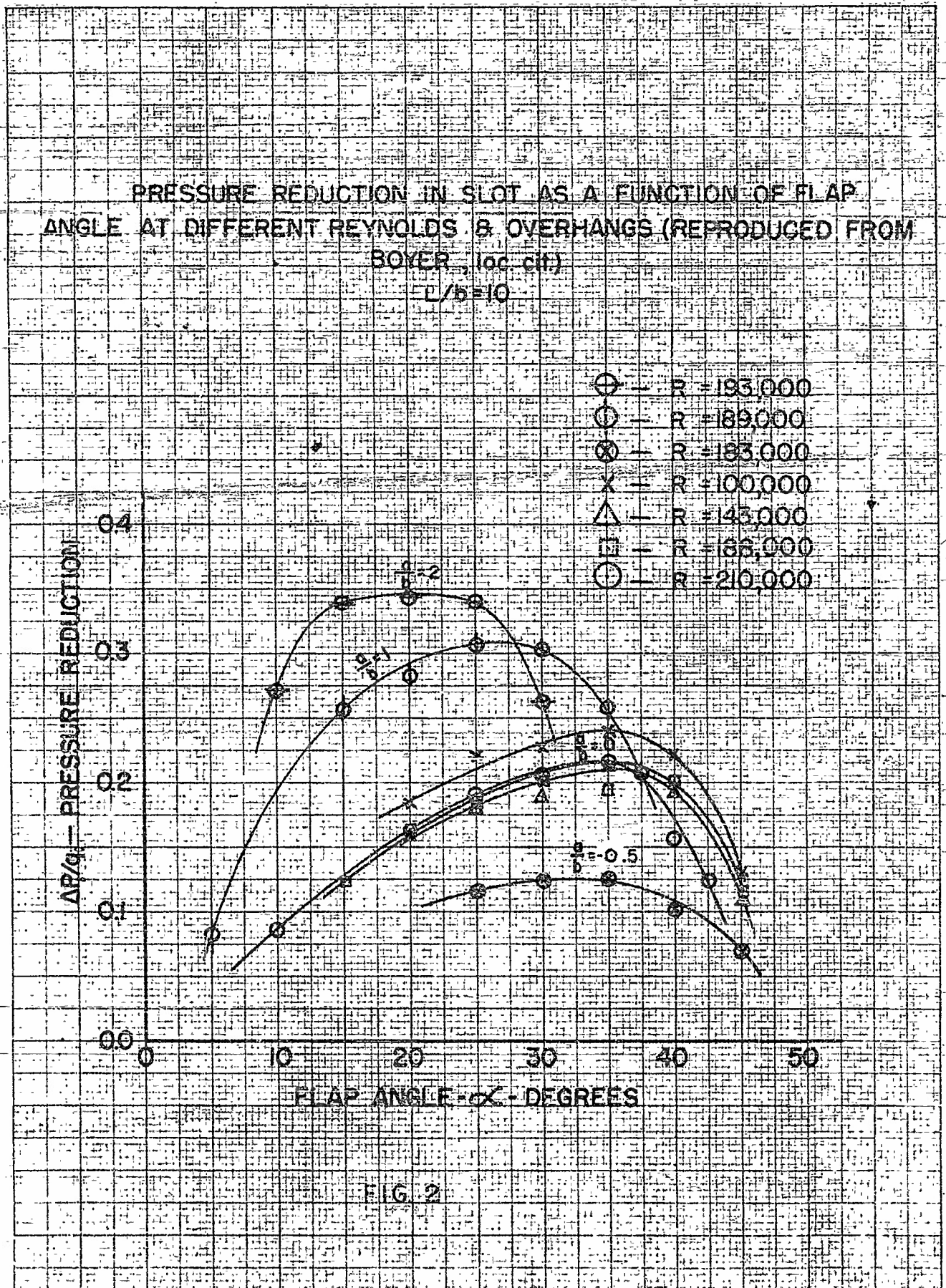

FIG 2

M. Coanda and Flight Lieutenant Sproule in October 1944. This report contained a detailed description of a Coanda nozzle and the results of some tests conducted with this nozzle. Other applications discussed in this report were a hydraulic propulsion system and a vacuum pump, which Coanda claimed developed a 99.8 per cent vacuum at a 98 per cent efficiency. A second report (5) by Flight Lieutenants Sproule and Adderly described work conducted by Chaussons Motor Company on a nozzle operating on exhaust gases from an internal combustion engine and used to draw cooling air through its radiator. The Chaussons Motor Company claimed to have obtained a twenty-to-one by-pass ratio, which is the ratio of cooling air to exhaust gases. A report by Lieutenant Robinson repeated much of the work presented in the previous two reports.

Professor Metral (1) concluded his theoretical report with results of tests of a series of internal combustion engines fitted with Coanda mufflers. These mufflers functioned very effectively in reducing the noise level produced by the exhaust gases and also improved engine performance by reducing the pressure in the exhaust manifold. Tests conducted on a one-cylinder motorcycle engine showed that use of the Coanda muffler resulted in an optimum power increase of 53 per cent. Further tests on various engines indicated a reduction in the brake specific fuel consumption, a reduction of 20 per cent being reported. Some additional applications were cited by Voedisch (7). They included a jet-induced wind tunnel and a wing reported to have a low drag coefficient and a high lift coefficient.

EXPERIMENTAL INVESTIGATION

The literature survey indicated a need for experimental work to determine the entrainment characteristics and "efficiency" of the Coanda effect. For an evaluation of the pressure reducing qualities of the effect such an efficiency can be expressed as

$$\eta_P = \frac{v \Delta P_1 G}{E_1} = \frac{\Delta P_1}{q_1}$$

Variations of this ratio have been studied by Boyer (2) and are discussed on page 10. No such expression could be determined as a measure of the efficiency of entrainment. Energy changes were thus considered by defining the so-called energy ratio as the ratio of the rate of flow of kinetic energy along the flap to the rate of flow of kinetic energy at section one in the slot. Entrainment was studied through the introduction of the mass-rate ratio, which was defined as the ratio of the mass rate of flow at any section along the flap to the mass-rate of flow in the slot. For a single flap these ratios were believed to be dependent upon the overhang, a; the flap length, L; the slot height, b; the velocity of the fluid in the slot, V_1; the viscosity and density of the primary fluid, μ_1 , and ρ_1 ; the viscosity and density of the surrounding medium, μ_2 and ρ_2 ; the flap angle, α ; and the distance along the flap to the section at which the energy and mass-rate ratios were defined. Compressibility effects were neglected.

A dimensional analysis of these variables indicated that the following relations exist:

$$m = f\left(\frac{a}{b}, \frac{L}{b}, R_1, \frac{\rho_2}{\rho_1}, \frac{\mu_2}{\mu_1}, \alpha, \frac{x}{b}\right) \qquad (1)$$

and

$$e = g\left(\frac{a}{b}, \frac{L}{b}, R_1, \frac{\rho_2}{\rho_1}, \frac{\mu_2}{\mu_1}, \alpha, \frac{x}{b}\right) \qquad (2)$$

Work by Thomas (8) with free jets has cited the importance of the ratio ρ_2/ρ_1.

The present investigation has been limited to conditions in which the densities and viscosities of the primary fluid and the surrounding medium were identical. The effect of flap length has been clearly discussed by Metral (1) and found to be of prime importance in determining the conditions for detachment of the jet. Work by the author also indicated the importance of L/b in determining the energy and mass-rate ratios. In the present investigation, however, the flap length was held constant at L/b equal to 14. Equations 1 and 2 for the conditions of the present experimental work could, therefore, be expressed as

$$m = F\left(\frac{a}{b}, R_1, \alpha, \frac{x}{b}\right)$$

$$e = G\left(\frac{a}{b}, R_1, \alpha, \frac{x}{b}\right)$$

Thus the work reported herein was undertaken to study the effects of overhang, Reynolds number, and flap angle upon the energy and mass-rate ratios at different points along the flap.

DESCRIPTION OF APPARATUS

To achieve the ends of the previous section, an experimental apparatus utilizing air as the primary and secondary mediums was constructed. This apparatus is shown in Figures 3 to 6. Air was supplied to a test section through a four-inch standard pipe by two Roots blowers operating in parallel. A large surge tank located at the discharge of the blowers aided in dampening pulsations in the air flow. The flow converged from the pipe to a nozzle at the entrance to the test section in a sheetmetal transition. The velocity distribution in the test section was improved by wire screening located at the transition entrance and exit. The nozzle had a well rounded approach on all edges, giving the slot a constant 3/4 in. by four in. cross-section. The slot exit terminated in a sharp corner followed by a 10 1/2 in. flap. The corner was formed by the beveled edge of the flap and the terminal edge of one vertical slot wall. Leakage at this point was prevented by masking tape placed along the outer side.

The flow passage was bounded on the upper and lower sides by two horizontal walls four inches apart. The lower wall was rigidly supported by a table while a section of the upper was free to rotate in the horizontal plane about the corner formed by the vertical slot wall and flap. This movable upper wall contained five parallel slots 1/16 in. in thickness and spaced at 1 1/2 in. intervals. The purpose of the slots was to permit total and static pressure traverses to be taken in sections at right angles to the flap. The flap was rigidly braced to the upper wall at right angles in such a manner to be also at right angles to the five slots.

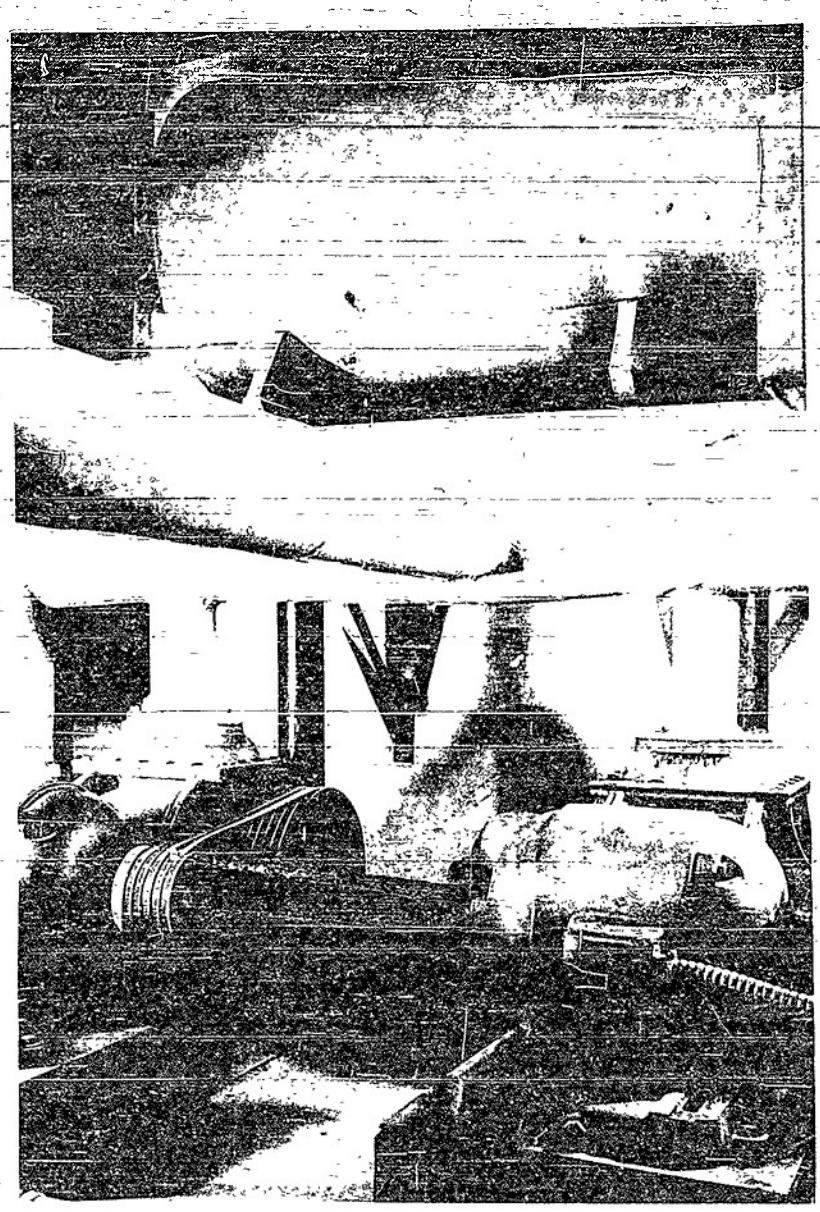

Fig. 3. View of Blower Installation

SECTIONAL DRAWING OF COANDA SLOT AND FLAP

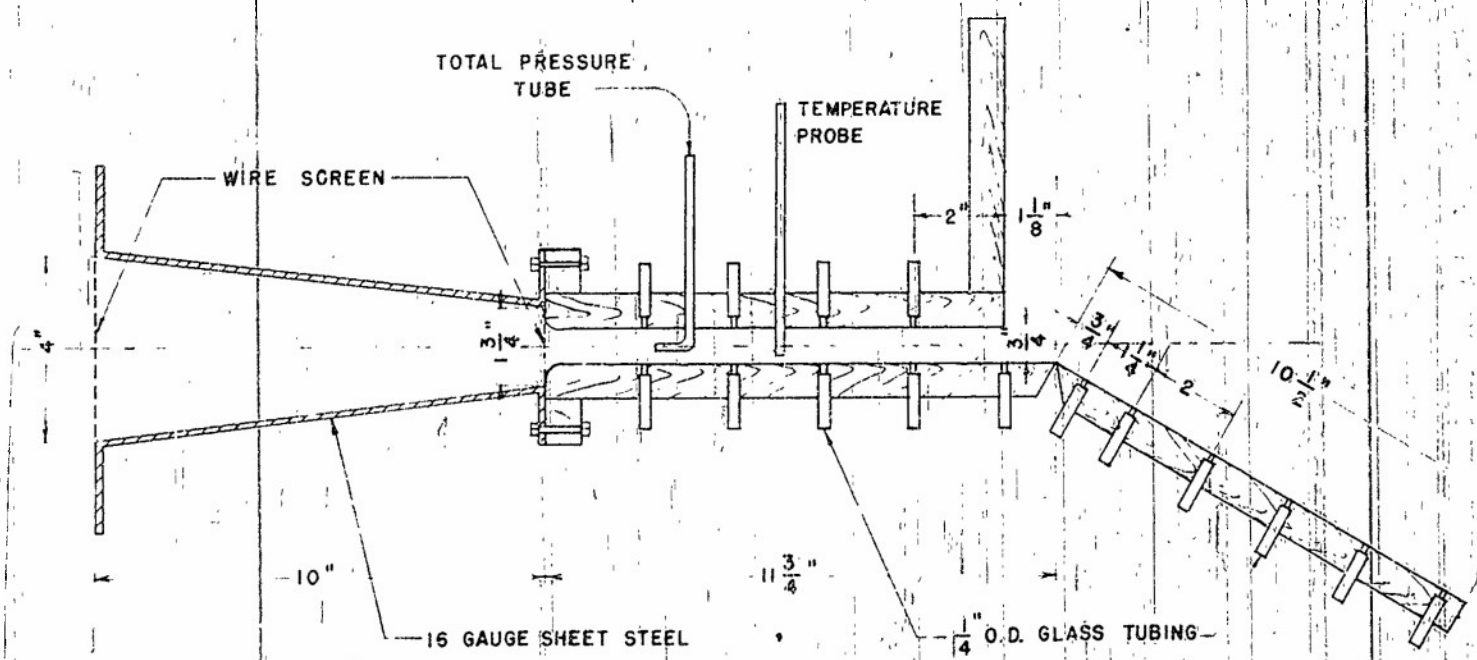

ALL WOODEN PARTS — WHITE PINE PLANED TO 1/4" THICK.

ALL STATIC PRESSURE HOLES 1/16" DIAMETER.

FIG. 4

Fig. 5. Top View of Test Section

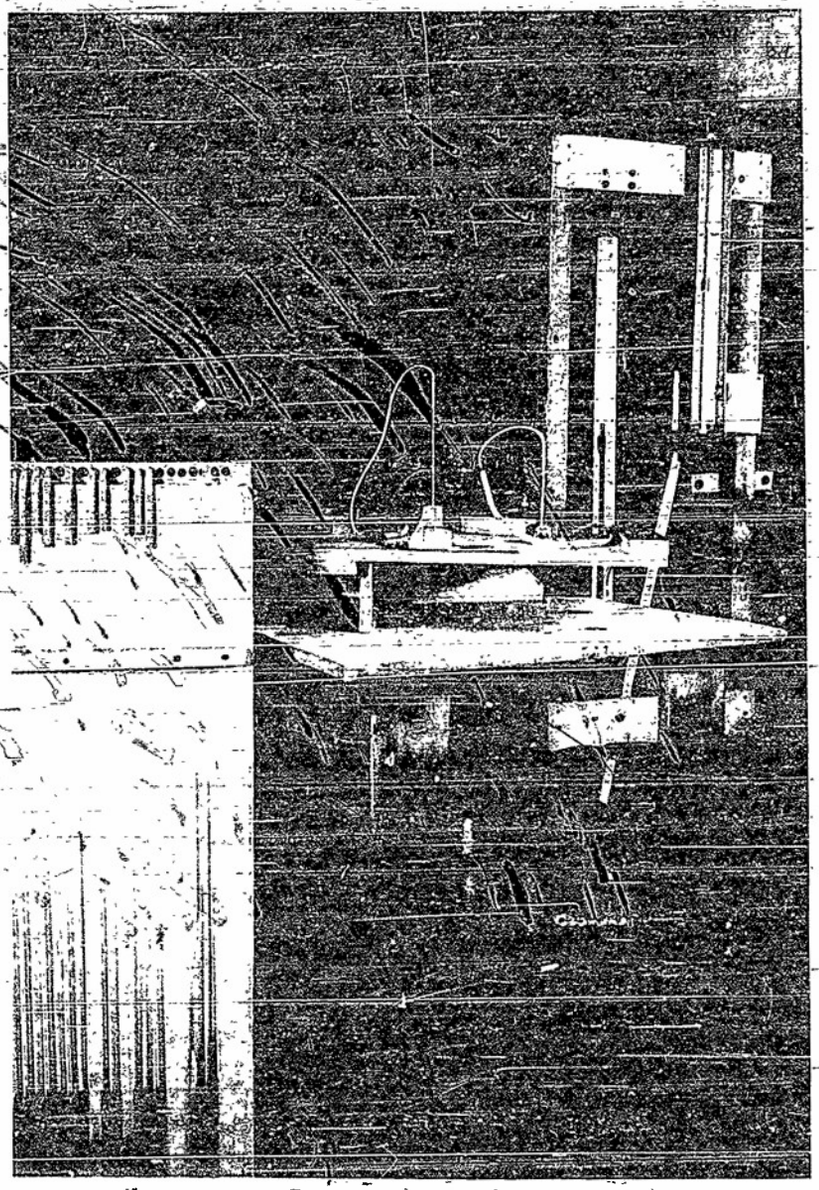

Fig. 6. Side View of Test Section

One edge of the upper wall was cut to form the arc of a circle eight inches in radius and having its center at the flap corner. This arc was made to fit a similar concave arc forming the remainder of the upper wall. This construction made it possible to vary the flap angle while keeping the slots at right angles to the flap.

A grid constructed on the upper face of the top wall permitted orientation of the total and static pressure tubes. A six-inch-radius protractor located on this same face and a fixed index made direct measurement of the flap angle possible. The entire test section was constructed of white pine planed to 3/4 in. in thickness and finished with a coat of shellac and two coats of polishing wax. The movable wall was securely fixed at a given flap angle by three large "C" clamps.

Temperature measurements were made at a point in the horizontal mid plane and 6 1/2 in. from the nozzle entrance and at different points along the flap with two different temperature probes. Each probe was constructed of No. 30 iron-constantan thermocouple wire with glass insulation. The wire was closed in 0.093 in. outer diameter brass tubing as shown in Figure 7. A double throw switch was used to connect either probe to a precision type potentiometer. Room temperatures were obtained with a 220 F mercury thermometer located at the entrance to the blower-intake duct.

Static pressures were obtained at points marked in Figure 4 through 1/16 in. diameter holes drilled in the passage walls. These pressures were measured with a water-filled multiple bank manometer which was vented to the atmosphere. Static pressure traverses in the sections perpendicular to the flap were made with a probe constructed of

0.060 in. O.D. stainless steel tubing as shown in Figure 7. In use it was inserted in the slot following that at which the traverse was being made. This permitted measurement at the correct section, for the static pressure hole was located 1 1/2 in. from the tube stem. The tube was connected through 1/4 in. rubber tubing to the pressure manifold shown in Figure 5. This was in turn connected to a water-filled manometer and a mercury-filled manometer connected in parallel, allowing accurate measurement of pressure over an extremely large range. Further description of these manometers can be found in the tabulation at the end of this section.

The total pressure five inches downstream from the nozzle entrance and in the horizontal mid-plane was obtained with an "L" head impact tube constructed of 0.06 in. O.D. brass tubing. The total pressure and flow direction at sections perpendicular to the flap were obtained with the direction-finding tube shown in Figures 5 and 7. This tube was constructed of 0.049 in. O.D. stainless steel tubing and had a No. 76 drill hole located 3/8 in. from the tube end. This permitted measurement of the total pressure in a plane 5/8 in. above the horizontal mid-plane. The tube was fitted with a pointer as shown in Figure 5 and was passed through the hole at the center of a three-inch protractor into the specified traversing slot. Measurement of the flow direction, ϕ , was obtained by rotating the tube and pointer to the right until the manometer indicated the static pressure which had been previously ascertained to exist at that point. The angle θ_R between a line perpendicular to the flap and the line subtended by the pointer was recorded, and the process repeated to the left. The angle

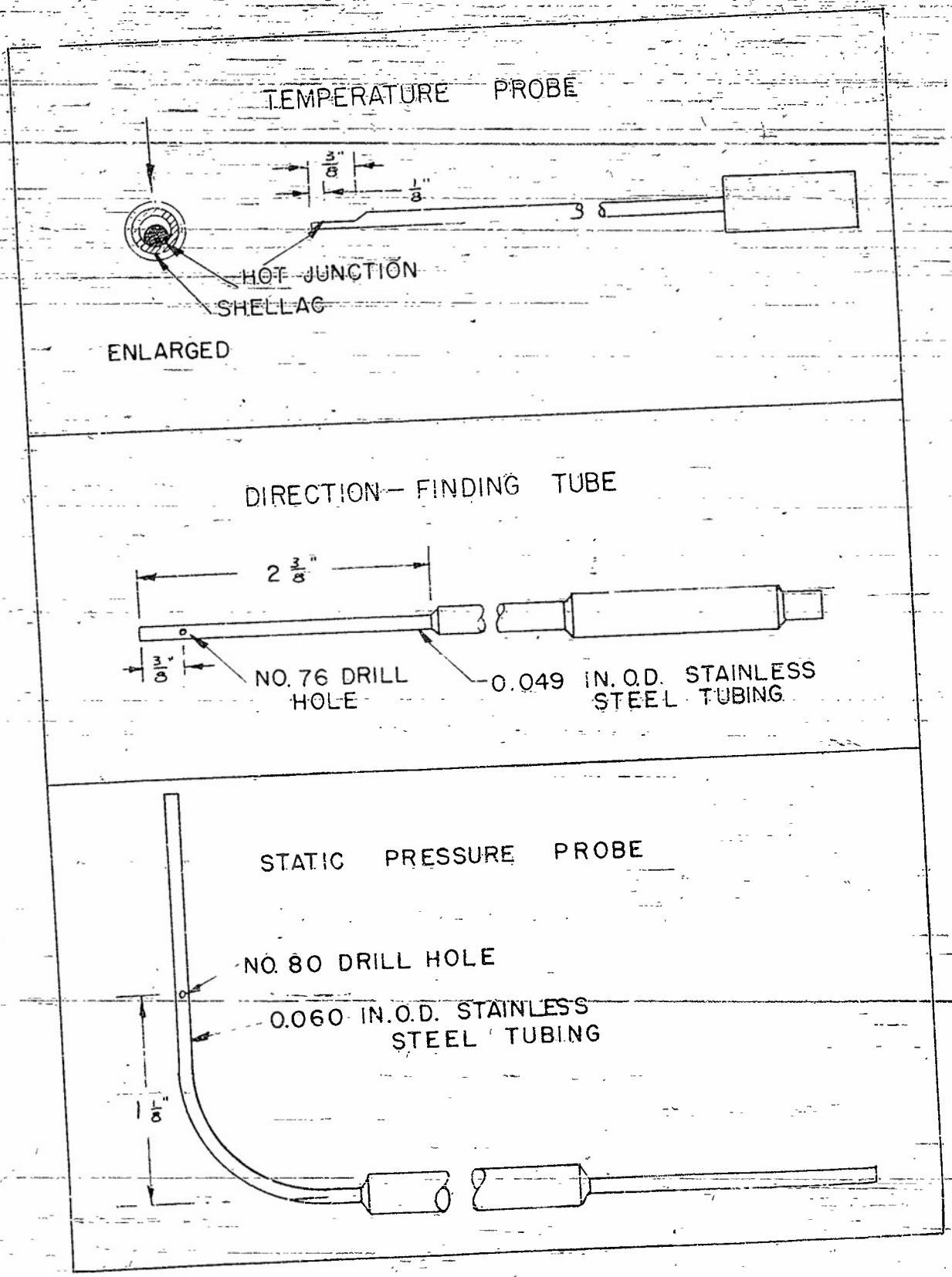
TEMPERATURE PROBE
3/8"
1/8"
HOT JUNCTION
SHELLAC
ENLARGED
DIRECTION-FINDING TUBE
2 3/8"
3/8"
NO. 76 DRILL HOLE
0.049 IN. O.D. STAINLESS STEEL TUBING
STATIC PRESSURE PROBE
NO. 80 DRILL HOLE
0.060 IN. O.D. STAINLESS STEEL TUBING
1/8"

FIG. 7

$(\theta_R - \theta_L)$ was bisected, thus indicating the direction of flow at that point. The total pressure was obtained by turning the pointer in the direction of flow. Calibration of the tube in the slot, where the mean flow was known to be parallel to the walls, indicated the angle $(\theta_R - \theta_L)$ deviated from 100 degrees by less than two degrees for all velocities up to a Mach number of 0.6. Calibration also showed an extreme change in indicated pressure with a small change in the angle of the pointer. The change in indicated pressure with small angle changes increased appreciably with increasing velocities and made it possible to measure the flow direction to within two degrees.

Following is a tabulation of important equipment and instruments.

1. Roots Blowers
   Manufactured by Pottstown Blower Co., Pottstown, Pennsylvania.
   Capacity 400 cfm at 1700 RPM and 8 in. Hg. pressure or vacuum.
   Horsepower - 15.
   Serial No. of one blower 74216 (none available for second blower).

2. Induction Motors
   Manufactured by General Electric Co., Schenectady, New York.
   Model 5 K 326 D 24.
   Horsepower - 15.
   Volts 220/440, 60-cycles.
   Speed 1745 RPM.
   Serial Nos. 0 A 17113 and LY 12505.

3. Vertical Manometer - water filled
   Manufactured by Tremont Instrument Co.
   Range - 10 in. to 20 in.
   Serial No. 1740, Type 30 W.

4. Vertical Manometer - mercury filled
   Manufactured by Merriam Co.
   Range - 9 in. to -9 in.
   Type W, Model A-324.
   Serial No. 14553.

5. Mercury Thermometer
   Manufactured by Central Scientific Co.
   Range 220 F.
   Type 19235 A.

6. Portable Precision Potentiometer
Manufactured by Leeds and Northrup Co.
Serial No. 347005.

7. Polar Planimeter
Manufactured by Crosby Steam Gage and Valve Co.
Serial No. ME-516.

TEST PROCEDURE

Tests were first conducted to investigate the variations of the energy and mass-rate ratios along the flap at a specified condition. This condition was taken at a/b equal to zero and α equal to 35 degrees corresponding to the point of maximum pressure reduction for no overhang as found by Boyer (2). Complete total and static pressure traverses were taken at the five sections along the flap at three different Reynolds numbers. Having determined the effect of x/b on e and m for this condition, all further traverses were confined to the first and fifth slots, corresponding to x/b equal to six and 14 respectively.

Preliminary considerations indicated that for fully developed turbulent flow the variations in m and e with Reynolds number would be slight. To verify this reasoning, tests were conducted at α equal to 35 degrees and a/b equal to zero over a large range of Reynolds numbers. Reynolds number was varied from 60,000 to 190,000 by varying the velocity at Section 1 from 160 feet per second to 600 feet per second. The results obtained showed that m varied little beyond a Reynolds number of 160,000 while e tended only to level off at R_1 equal to 180,000. It was thus decided to conduct all further tests at R_1 equal to approximately 160,000, corresponding to a slot velocity of nearly 500 fps.

A complete set of tests was then conducted at this Reynolds number and no overhang while varying the flap angle from zero degrees to 40 degrees and taking traverses at x/b equal to six and 14 only. Tests were not conducted beyond a flap angle of 40 degrees because of the

strong possibility of detachment of the jet from the flap.

To determine the effects of overhang, α was held constant at 35 degrees and R_1 constant at 155,000, while the overhang was varied from 1 1/2 to 3. The overhang was varied by adding small blocks of wood of different lengths to the end of the vertical slot wall opposite the corner. These blocks were smoothly finished and held in place with wood screws.

Traverses were taken in planes parallel to the flap at the point of maximum velocity to determine the deviation in the flow from two-dimensional flow. This deviation was approximated by determining the difference between the velocity in the test plane indicated by these traverses and the mean velocity across the width of the jet. It was believed that a condition of two-dimensional flow might be completely invalidated by separation occurring along the horizontal walls. This effect had been previously noted by several investigators (3) in work with two-dimensional diffusers. The conditions at which these traverses were taken were the conditions at which a large pressure gradient, dp/dx, existed. This insured the existence of the greatest tendency toward separation. Tests at α equal to 35 degrees and no overhang indicated a satisfactory velocity distribution. Tests at α equal to 20 degrees and an overhang of 2 1/2 clearly indicated the existence of separation along the upper horizontal wall. Although it was the intention of the author to run complete tests at several overhangs, the existence of this separation at the angles of optimum pressure reduction at the higher overhangs made such tests impractical with the existing apparatus.

In conducting the tests, the blowers were run at the desired conditions for 15 minutes prior to taking data. Changes in the discharge velocity were made by opening an auxiliary gate valve connected to the surge tank.

Each complete traverse was conducted in two steps. The first was a static pressure traverse with the static pressure probe held parallel to the flap in the slot following that at which the traverse was being made. The second consisted of a total pressure traverse with the direction finding tube as previously described. Total pressure traverses at Section 1 in the slot showed that no appreciable change in velocity occurred across the entire slot height. The mean velocity of the flow in the slot was therefore obtained from a single total pressure measurement at the center of the slot and in the horizontal mid-plane.

The temperature at the point of maximum velocity at each section was determined with the flap-temperature probe. The temperature of the jet at that section was then assumed to be equal to the mean of this indicated temperature and room temperature.

Care was taken to cover all unused traversing slots and all cracks with masking tape. Leakage at the traversing slot in use was prevented by a fairly tight fit between the protractor and wall. Manometer readings were so taken as to prevent error due to parallax.

EXPERIMENTAL DATA AND CALCULATIONS

Data taken for each run included measurements of static pressures along the slot walls and flap at the beginning and end of each run. Recorded at the same time were the total pressure in the nozzle, the indicated temperature in the nozzle, and room temperature. The data taken during the traverses included static and total pressure readings at 0.2 in. intervals along the traversing slot. In the immediate vicinity of the flap these readings were taken at 0.1 in. intervals. The flow direction was recorded at 0.4 in. intervals while the indicated temperature of the jet was determined at only one point.

To calculate the mass-rate and energy ratios, the quantities $Z \cos \phi \sqrt{h_m}$ and $W \cos \phi \, (h_m)^{3/2}$ were plotted for each traverse against the distance from the flap. The integrals

$$\int_A Z \cos \phi \sqrt{h_m} \, dA \qquad \text{and}$$

$$\int_A W \cos \phi \, (h_m)^{3/2} \, dA$$

were then determined by measuring the area between these curves and their coordinate axes with a planimeter. The energy and mass-rate ratios were then calculated from

$$m = \frac{\left(\sqrt{\frac{p}{T_i}} \int_A Z \cos \phi \, (h_m)^{1/2} \, dA \right) x}{\left(b \, W \, Z \sqrt{\frac{p}{T_i}} \sqrt{h_m} \right)_1}$$

and

$$e = \frac{\left(\sqrt{\frac{T_i}{p}} \int_{Ax} w \cos\phi \, (h_m)^{3/2} \, dA\right)}{\left(b \, w \, W \sqrt{\frac{T_1}{p}} \, (h_m)^{3/2}\right)_1}$$

as derived in the appendix.

Results of all calculations were presented in graphical form. Experimentally determined velocity distributions were approximated by plotting $Z \cos\phi \sqrt{h_m}$ against distance from the flap. This quantity can be shown to be nearly proportional to the velocity.

DISCUSSION OF RESULTS

Accuracy of the results is limited by the non-two-dimensionality of the flow along the flap. The extremely high pressure gradient existing along the flap at the point of maximum pressure reduction for large overhangs was sufficient to cause separation to occur along the upper wall. This is illustrated in Figure 8 by the velocity distributions in planes parallel to the flap at the point of maximum velocity. Similar traverses taken at no overhang and at a flap angle of 35 degrees indicate a satisfactory distribution. The maximum deviation of the velocity in the test plane from the mean velocity across the width of the test section for this condition was approximately 10 per cent at x/b equal to six and three per cent at x/b equal to 14. Errors in determining the velocity were carried over in calculating the mass-rate of flow and the mass-rate ratio. In calculating the energy ratio, these errors were approximately tripled. Thus, the maximum deviation of the kinetic energy across the width of the test section was less than 30 per cent at x/b equal to six and less than nine per cent for x/b equal to 14. The condition of α equal to 35 degrees represents the condition of maximum deviation from two-dimensional flow for no overhang. At smaller flap angles this deviation was decreased.

Other errors incurred in the experimental procedure were almost insignificant in comparison to those discussed in the preceding paragraph. The errors resulting from pulsations in the blower discharge and from incorrect static pressure measurements across the jet would have been of importance had the flow been more nearly two-dimensional.

VELOCITY TRAVERSES IN PLANES PARALLEL TO FLAP AT R= 65,000

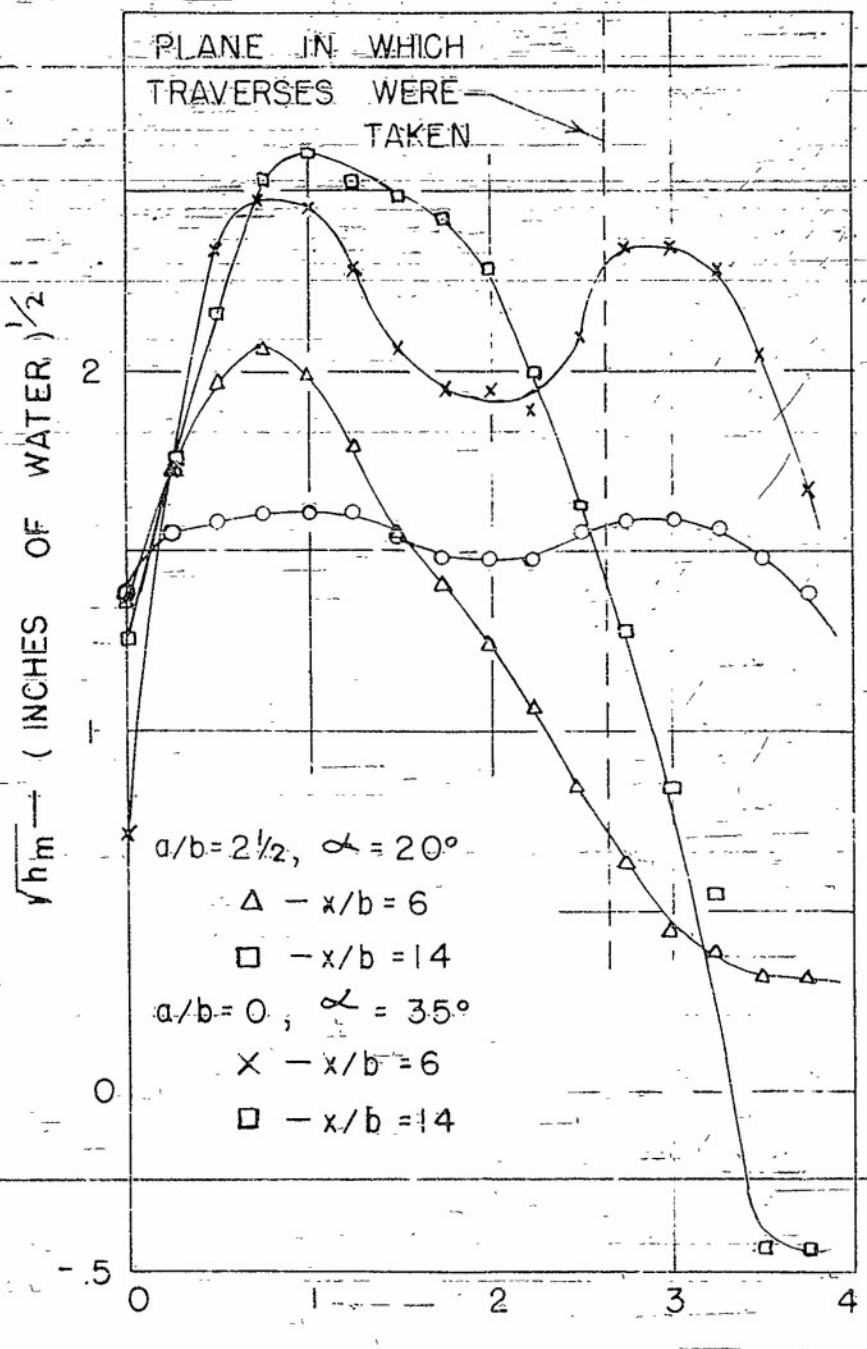

FIG. 8

One other error became evident in plotting the kinetic energy distributions for integration. These plots indicated that in making the traverses, insufficient measurements had been taken in the region of maximum velocity. This made it difficult to define the energy distribution curve and to determine accurately the corresponding integral. No such difficulty was experienced in defining the ρ V curve. The mean deviation of a series of planimeter readings for a given curve was less than one per cent.

CONCLUSIONS

Effect of Distance Along the Flap

Reference to Figure 9 indicates clearly the increase in the mass-rate of flow with increasing x/b. The decrease in the slope of the curves beyond x/b equal to six can be attributed in part to a decrease in the pressure reduction along the flap and in part to a decrease in the velocity gradient, dV/dy. For Prandtl (9) has shown that the turbulent shear stress between the jet and the surrounding medium can be expressed as

$$\tau = \rho l^2 \left| \frac{dV}{dy} \right| \frac{dV}{dy}$$

Thus any decrease in the velocity gradient will result in a corresponding decrease in the turbulent shear stress and in the entrainment due to turbulent momentum exchange. This decrease in dV/dy is shown clearly in the velocity profiles of Figure 11.

Prior to entering upon a discussion of the variations in the energy ratio, it will be advantageous to elaborate upon the energy changes along the flap. They may best be understood by dividing the flow through the slot, around the corner, and down the flap into two processes. These are an expansion process at the corner followed by a compression process down the flap. The first is characterized by an efficient conversion of pressure into kinetic energy; the second, by an inefficient conversion of kinetic energy into pressure. Losses occurring in this second process are due to a dissipation of kinetic

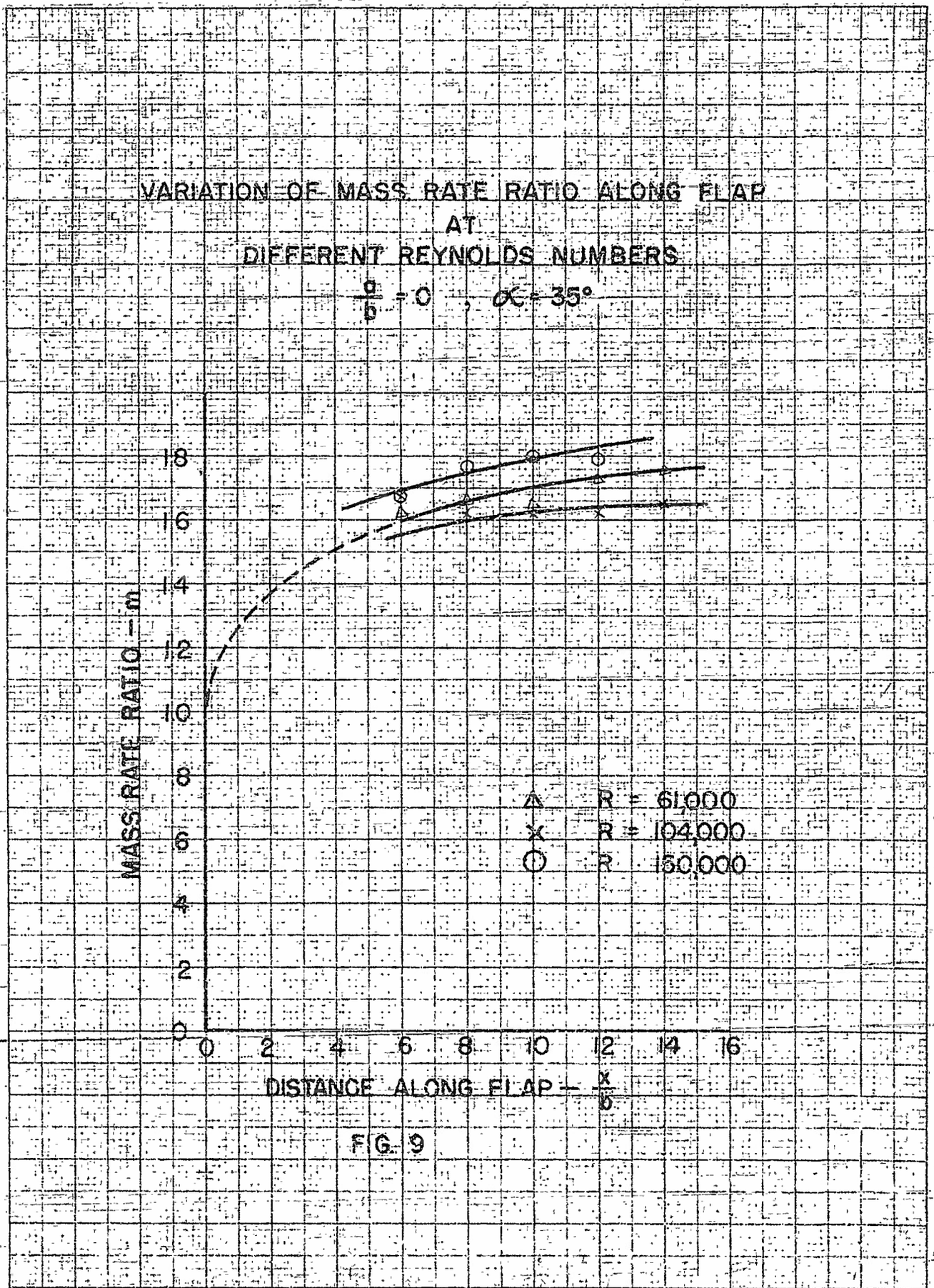
VARIATION OF MASS RATE RATIO ALONG FLAP
AT
DIFFERENT REYNOLDS NUMBERS
$\frac{a}{b} = 0$, $\alpha = 35°$
MASS RATE RATIO – m
0
2
4
6
8
10
12
14
16
18
0
2
4
6
8
10
12
14
16
DISTANCE ALONG FLAP – $\frac{x}{b}$
△ R = 61,000
× R = 104,000
○ R = 150,000

FIG. 9

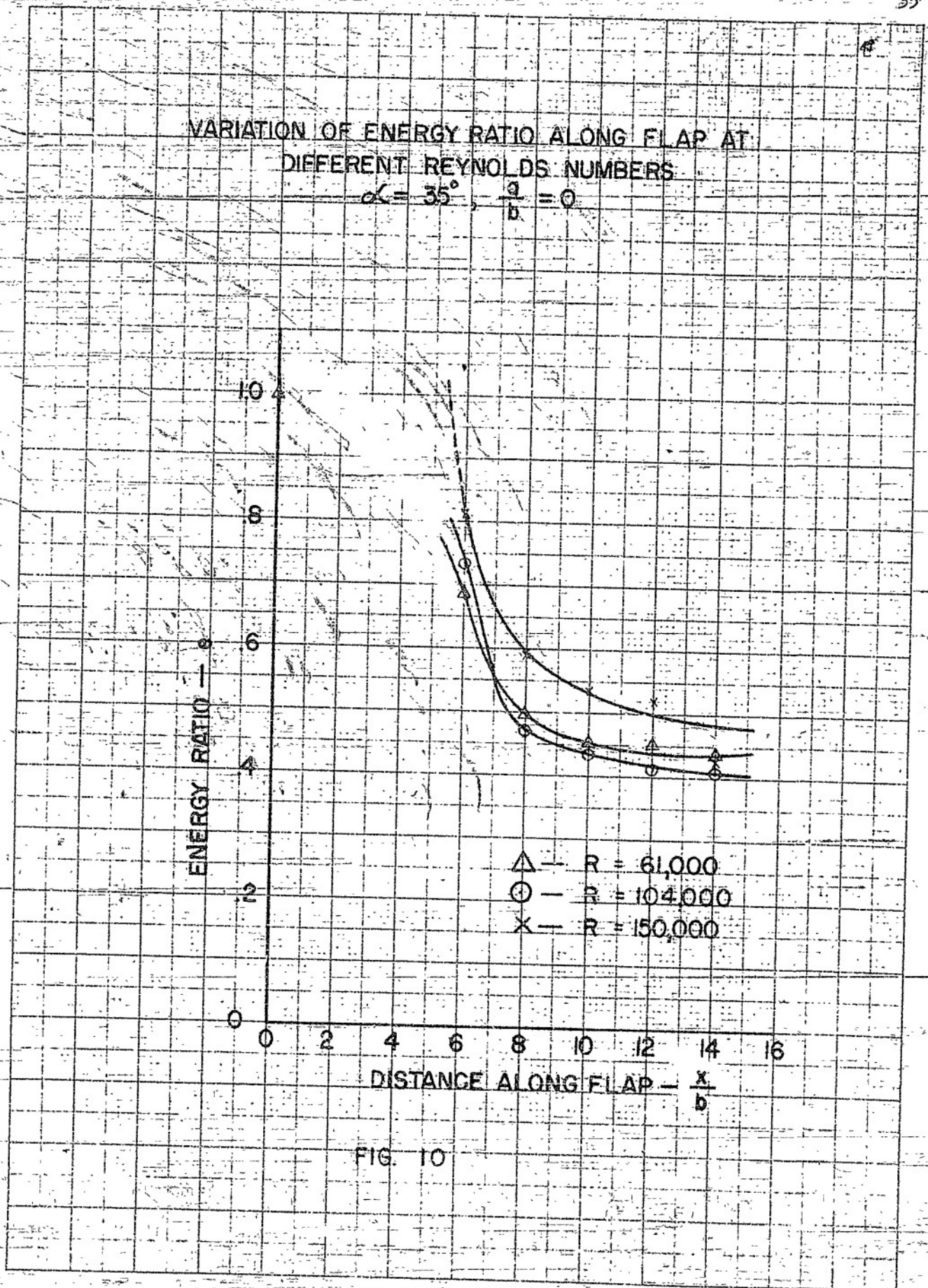
VARIATION OF ENERGY RATIO ALONG FLAP AT DIFFERENT REYNOLDS NUMBERS
$\alpha = 35°$, $\frac{a}{b} = 0$
ENERGY RATIO — $\frac{e}{q}$
1.0
.8
.6
.4
.2
0
0
2
4
6
8
10
12
14
16
DISTANCE ALONG FLAP — $\frac{x}{b}$
△ — R = 61,000
⊙ — R = 104,000
X — R = 150,000

FIG. 10

VELOCITY DISTRIBUTION AT DIFFERENT SECTIONS ALONG THE FLAP $\alpha = 35°$, $a/b = 0$, $R = 150{,}000$

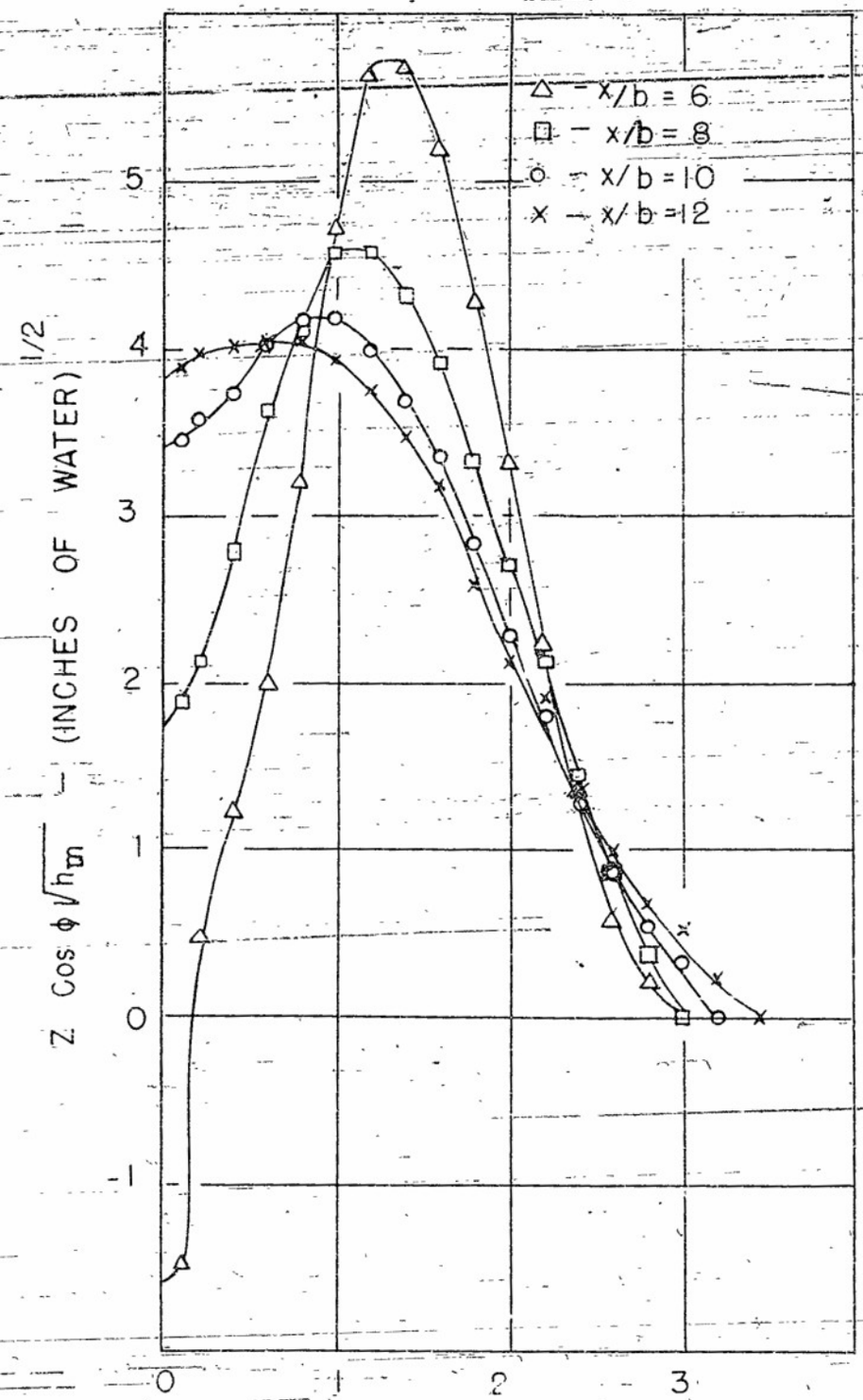

FIG. 11

energy into unavailable thermal energy because of turbulent shear stresses, while under certain other conditions this loss is greatly augmented by the existence of a large region of separation along the flap. The chief factor determining this separation is a large pressure gradient, dp/dx, along the flap. The pressure gradient in turn is determined by the overhang and the flap angle. According to Pfleiderer (10) the losses due to compression of an air stream in a diffuser are proportional to the sine of the angle of divergence. Similarly, losses in the compression process along the flap can be expected to increase with increasing flap angle.

Referring now to Figure 10 it can be seen that the kinetic energy of the jet decreases appreciably along the flap. This decrease becomes particularly large between the corner and x/b equal to eight. This region is further characterized by a large increase in the pressure, p_x. Thus, the decrease in the energy ratio can be attributed mainly to work done by the fluid against the rising pressure along the flap. The following losses also contribute to the reduction in e : (a) losses in the region of separation, (b) losses in the boundary layer along the flap, and (c) losses due to high turbulence in the mixing zone between the jet and the surrounding medium. Beyond x/b equal to eight separation no longer exists and the pressure gradient is small. Thus, the energy ratio decreases at a less rapid rate. In application it would be impossible to utilize a short flap to achieve the high energy ratios; for, as explained by Metral (1), the pressure of the stream at the end of the flap must be nearly equal to that of the surrounding medium. Thus the high energy ratios will always be reduced

because of the work done against the rising pressure.

Effect of Reynolds Number

Figure 12 indicates a definite increase in the mass-rate ratio with increasing Reynolds number. This can be attributed solely to an increase in the turbulent momentum exchange between the jet and the surrounding medium.

Traverses taken at x/b equal to six and at the conditions of Figure 12 show a slight tendency toward thickening of the region of separation with increasing Reynolds number. It is therefore probable that the apparent increase in kinetic energy shown in Figure 12 was not due to a decrease in the losses in the region of separation.

Effect of Flap Angle

Figure 13 shows an increase in the mass-rate ratio for x/b equal to six up to a flap angle of 35 degrees. Beyond this point there is a decrease in the mass-rate ratio. Insufficient time prohibited further tests in this region, but a decrease in the mass-rate ratio at this point could be predicted from the tests of Boyer. His results, reproduced in Figure 2, show a drop in the pressure reduction for no overheng beyond a flap angle of 35 degrees. It has been previously explained that entrainment of the surrounding medium by the jet is in part due to the pressure reduction in the jet.

For x/b equal to 14 there is no apparent drop in the mass-rate

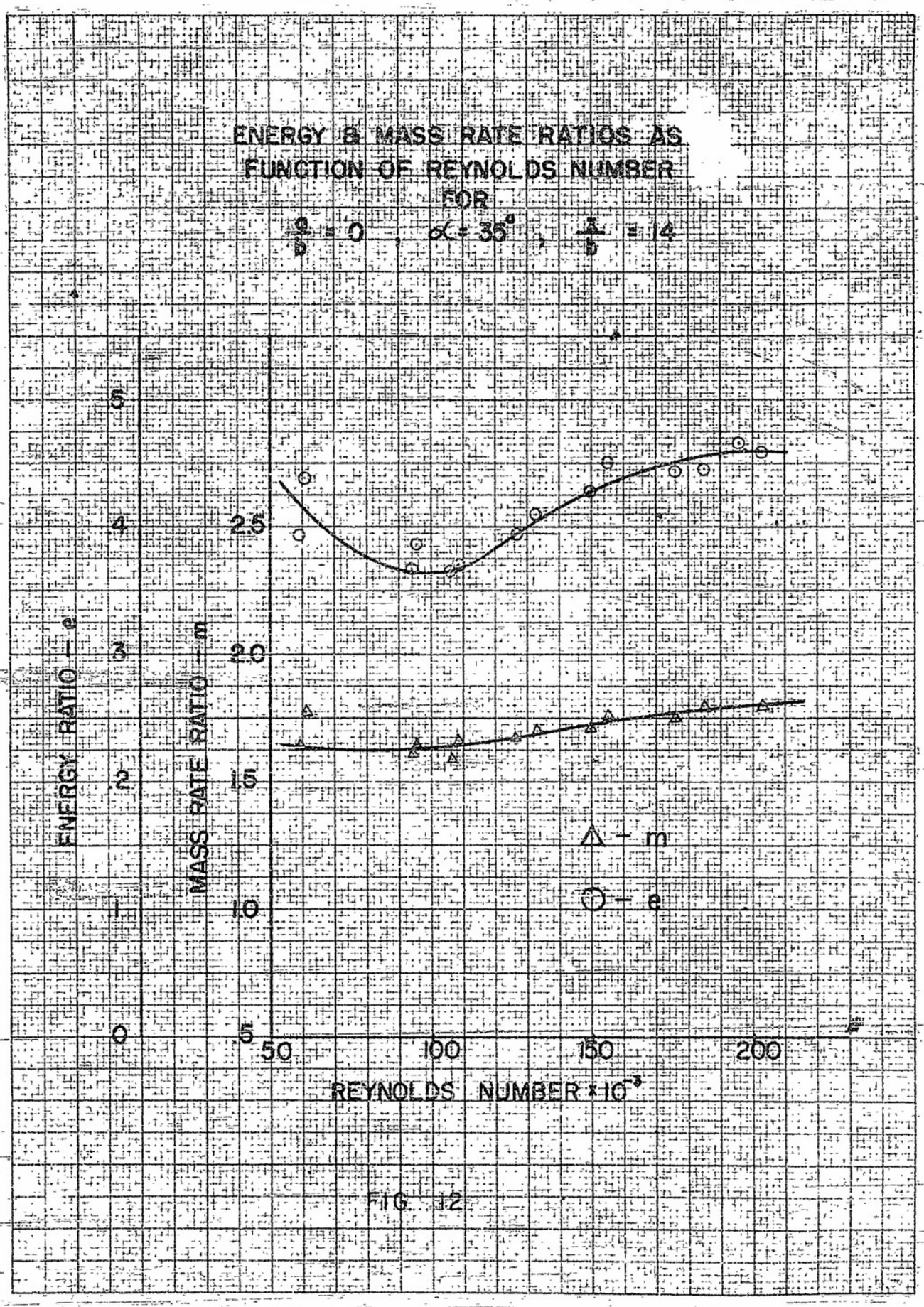
ENERGY & MASS RATE RATIOS AS
FUNCTION OF REYNOLDS NUMBER
FOR
$\frac{a}{b} = 0$, $\alpha = 35°$, $\frac{A}{b} = 14$
ENERGY RATIO — e
MASS RATE RATIO — m
REYNOLDS NUMBER x 10^{-3}
Δ - m
○ - e
0
1
2
3
4
5
1.0
1.5
2.0
2.5
50
100
150
200

FIG 12

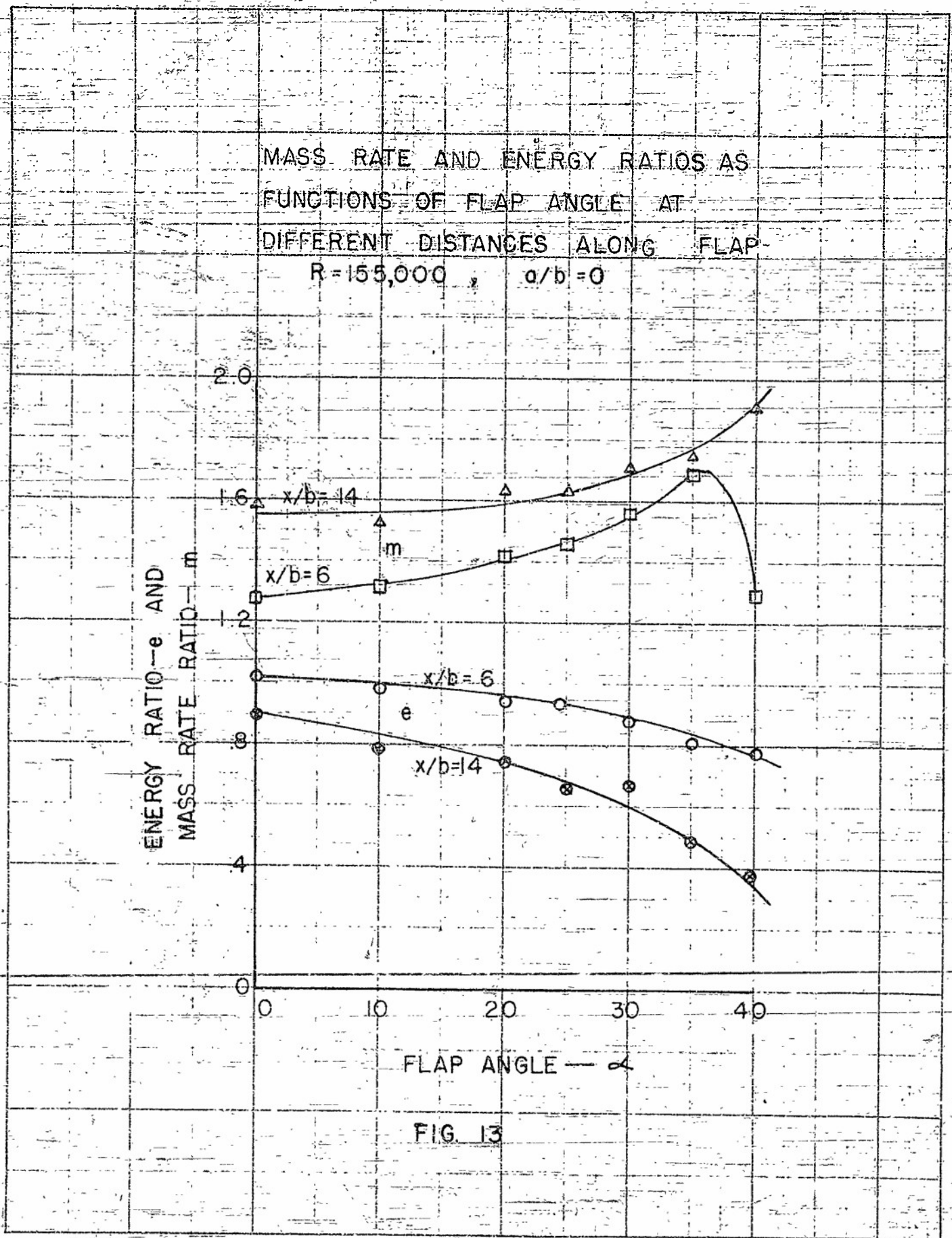

FIG 13

ratio over the entire range of flap angles at which tests were conducted. This is possibly due to a lengthening of the region of low pressure within the jet in spite of the decrease in the pressure reduction. It is of importance to note that the mass-rate ratio for x/b equal to 14 and α equal to zero degrees has a value of 1.55. This value is only 20 per cent less than the peak value of the mass-ratio determined by this series of tests at no overhang. This can be attributed to the extremely high velocity gradient, dV/dy, existing along the outer surface of the jet. Increasing the flap angle, while increasing the pressure reduction, results in a decrease in the velocity gradient, dV/dy, along the outer surface of the jet, and also in an increase in the rate at which the jet widens. This decrease in dV/dy results in a decrease in the turbulent momentum exchange between the jet and the surrounding medium. Thus at higher flap angles the increase in entrainment due to larger pressure reductions is partly offset by a decrease in the entrainment resulting from turbulent momentum exchange.

With increasing flap angles the energy ratio decreases rapidly. This is due entirely to an increase in the losses in the region of separation. Definite proof of the increase in these losses is given by the velocity profiles presented in Figure 14. The increase in the thickness of the region of separation with increasing flap angles is evident. It is important to note the extremely large increase in this thickness that occurs as the angle of detachment of the jet is approached.

VELOCITY TRAVERSES AT VARYING ANGLES
FOR a/b=0, x/b=6, R=155,000

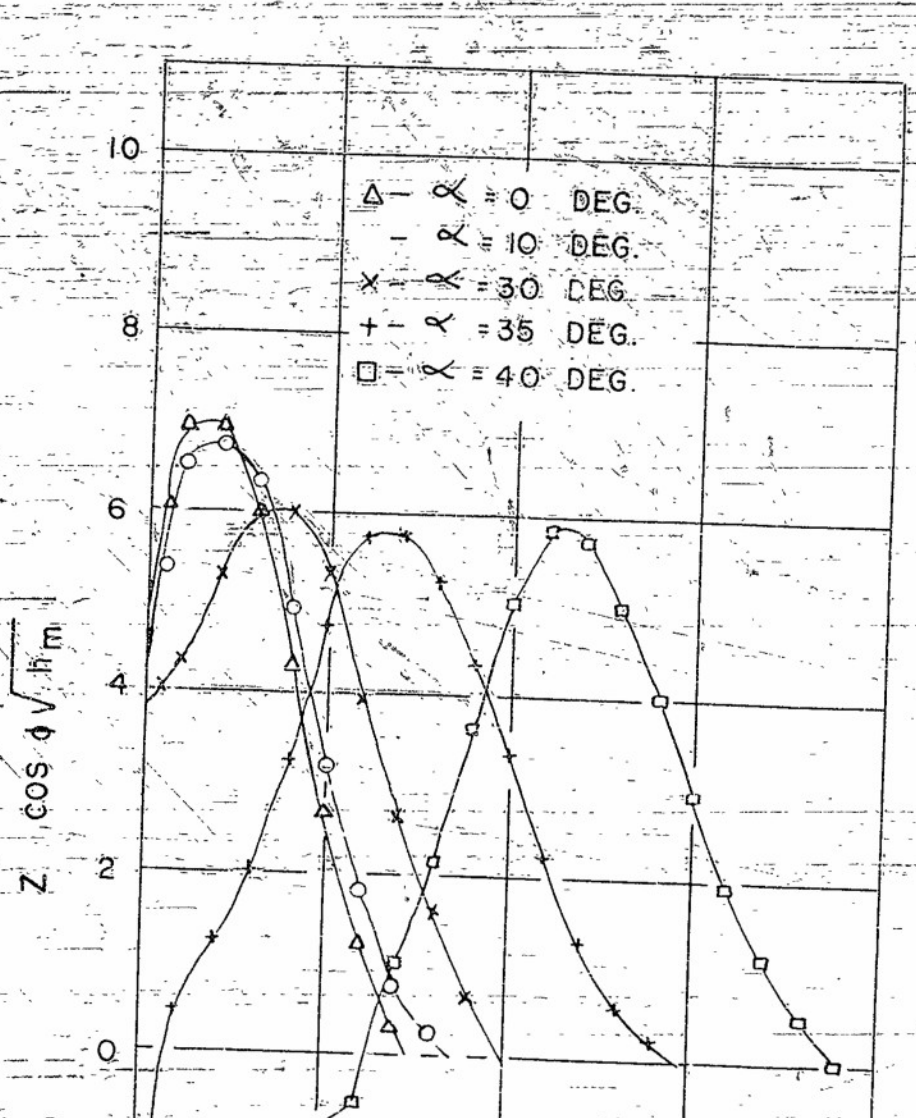

FIG. 14

Effect of Overhang

The results presented in Figure 15 show the variation of e and m with overhang at a fixed flap angle of 35 degrees. Both curves of mass-rate ratio indicate a maximum exists which m decreases with increasing overhang.

The energy ratio curves show that e increases slightly with increasing overhang. No plausible explanation for this increase can be offered. In fact, velocity profiles presented in Figure 16 show that the region of separation increases rapidly with increasing overhangs. This indicates that the losses due to separation should also increase rapidly. But such an increase would result in a reduction in the kinetic energy of the jet, thus contradicting the results of Figure 15. The increases in e with increasing overhang are small, however, and may even be within the experimental error.

Summary of Conclusions

1. The mechanism of entrainment is equally dependent on the pressure reduction in the jet and turbulent momentum exchange in the mixing zone.

2. Reductions in kinetic energy along the flap are due to the following in order of significance:

   (a) Work done by the stream against rising pressure along the flap

   (b) Losses in the region of separation

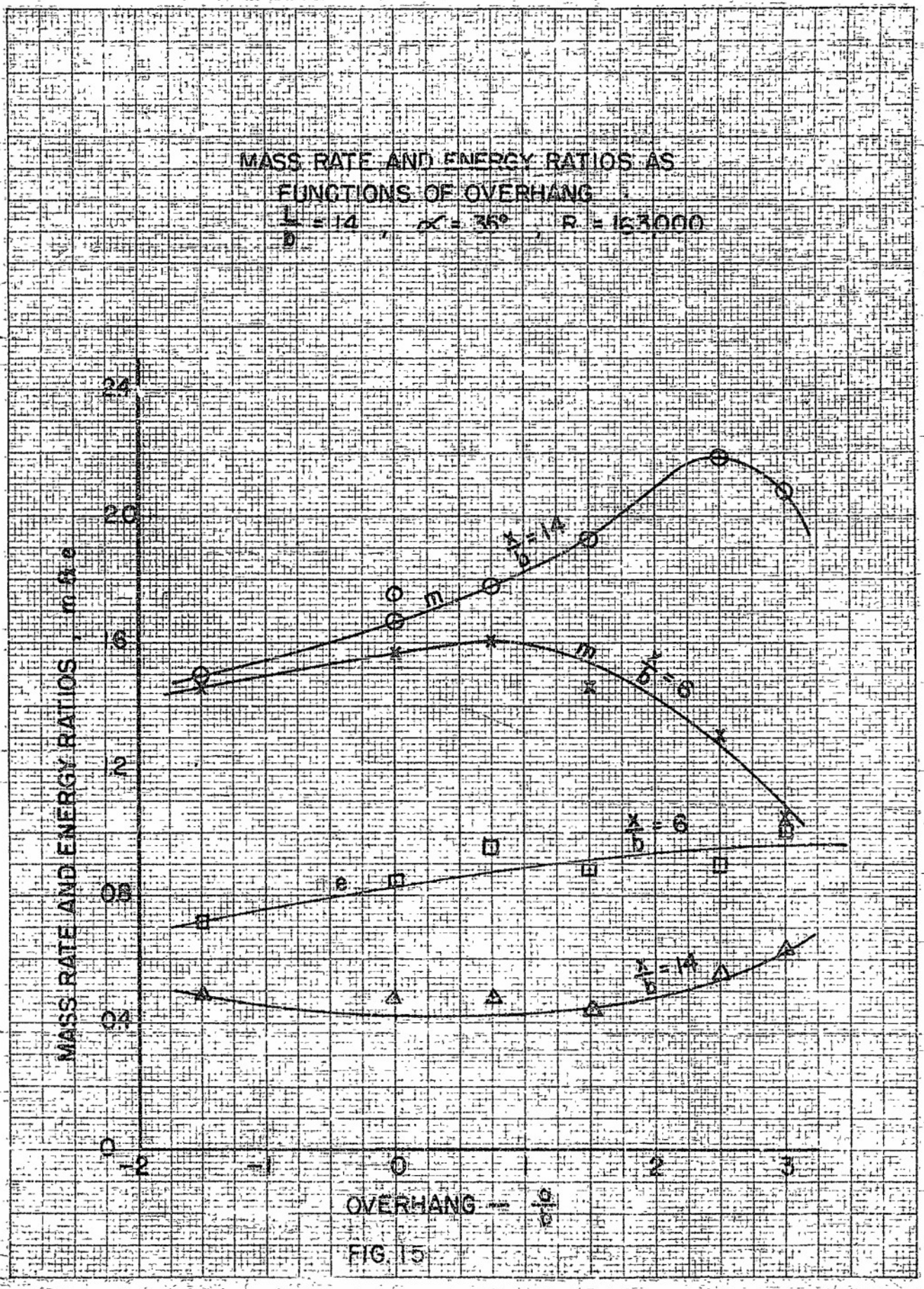
MASS RATE AND ENERGY RATIOS AS
FUNCTIONS OF OVERHANG
$\frac{L}{D} = 14$, $\alpha = 36°$, $R = 153000$
MASS RATE AND ENERGY RATIOS , m & e
OVERHANG — $\frac{o}{D}$
m
e
$\frac{L}{D} = 14$
$\frac{L}{D} = 6$
$\frac{L}{D} = 0$
2.4
2.0
1.6
1.2
0.8
0.4
0
-2
-1
0
1
2
3

FIG. 15

VELOCITY DISTRIBUTIONS FOR DIFFERENT OVERHANGS.
$\alpha = 35°$, $x/b = 6$, $R = 166{,}000$.

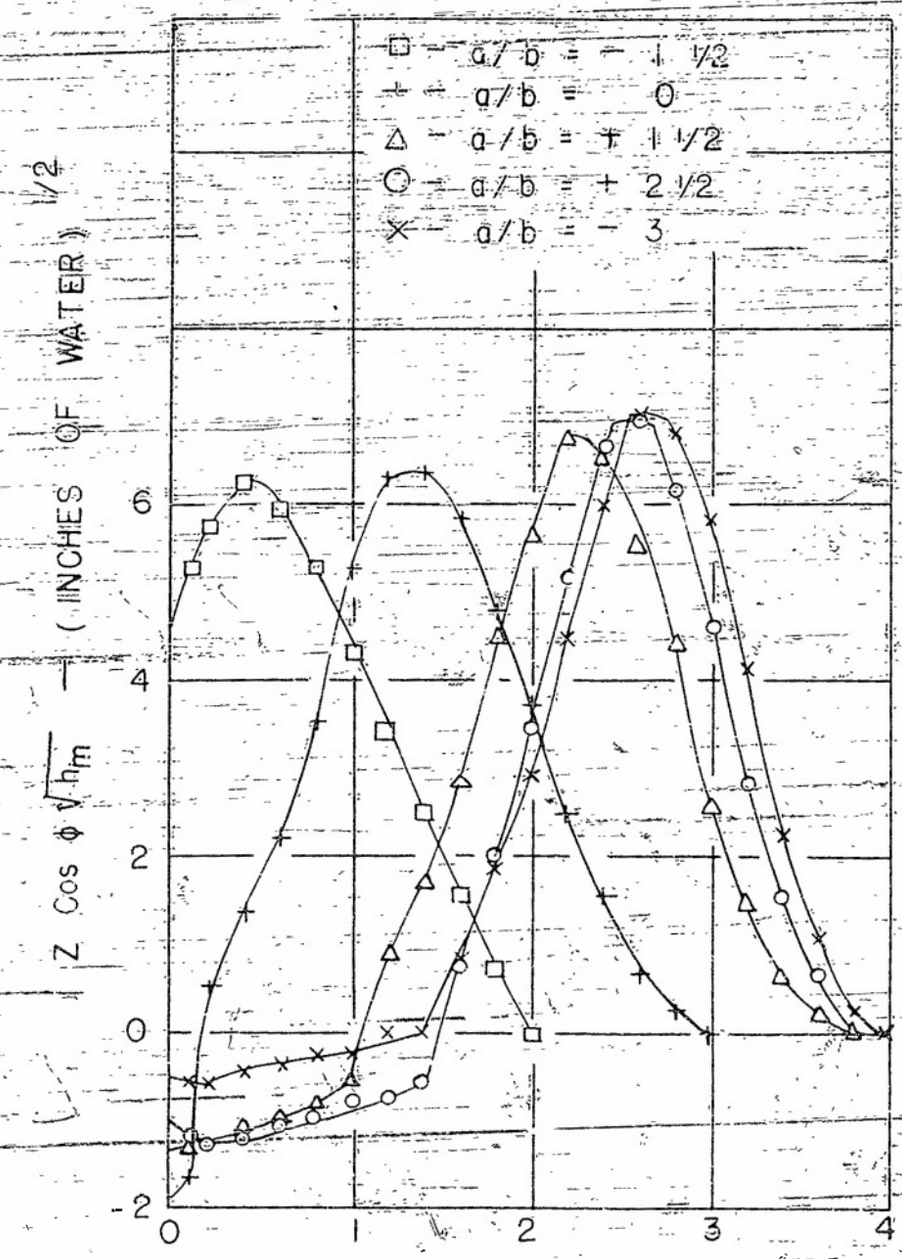

FIG. 16

(c) Losses in the boundary layer

(d) Losses due to the high turbulence in the mixing zone

3. Higher mass-rate ratios may be obtained by increasing the overhang. This, however, will be accomplished at the expense of a decrease in the energy ratio.

BIBLIOGRAPHY

1. A. R. Metral, "Method of Increasing Fluid Stream by Diverting It From Its Axis of Flow. Coanda Effect", U.S.A.A.F. Translation, Report No. F-TS-823-R.E. Also published as "Sur un Phenomene de Deviation des Veines Fluides et Ses Applications. Effet Coanda", Proceedings of Fifth International Congress for Applied Mechanics, Wiley and Sons, pp. 456 - 466. Discussion by John R. Weske.

2. I. J. Boyer, "Preliminary Investigation of the Coanda Effect", U.S.A.A.F. Technical Report (Preprint), Report No. F-TR-2155-ND.

3. A. S. Hall, "Investigation of Separation in Two-Dimensional Flow", Thesis No. 10719, Purdue University.

4. F/Lt. R. S. Sproule, "Report on Interrogation of M. Henri Coanda and Visit to Societe Coanda, Paris", Wright Field Document D 52.420/27.

5. F/Lt. R. S. Sproule and F/Lt. Adderley, "Report of Visit to Paris", Wright Field Document D 52.420/27.

6. S. T. Robinson, Lt. U.S.N.R., "Interrogation of M. Henri Coanda", also Mission Report No. 45, Wright Field Document D 52.420/27.

7. A. Voedisch, "Analytical Investigation of the Coanda Effect", Wright Field Report No. F-TR-2155-ND (Preprint).

8. J. Thomas, "Entrainment of Air by a Jet of Gas", Phil. Magazine (6) 47, pp. 1048 - 1056, 1924.

9. L. Prandtl, "Aerodynamic Theory" edited by W. F. Durand, Vol. III, Div. G, p. 128.

10. "Aerodynamic Theory", edited by W. F. Durand, Vol. III, Div. I, p. 272.

ADDITIONAL REFERENCES

1. "Induced Air Flow for Engine Cooling", Automotive and Aviation Industries, Feb. 15, 1946, pp. 30, 31.

2. "Augmented Flow", Flight, Aug. 15, 1946.

3. "Coanda Effect", American Helicopter, August 1946.

4. E. Forthmann, "Turbulent Jet Expansion", U. S. National Advisory Committee for Aeronautics, Technical Memorandum 789.

APPENDIX

CALCULATIONS

Derivations of all formulae required in making the necessary calculations are herein presented. All derivations are based on the following assumptions: (a) the flow is isentropic; (b) the fluid follows the perfect gas relations; (c) the specific heat ratio and gas constants have values of 1.40 and 53.3 ft-lb/lb-°R respectively.

Compressibility Factors

Velocity measurements were made by the determination of total pressure, p_T; static pressure, p; and indicated temperature, T_i. Calculation of velocity then followed from the Saint-Venant equation,

$$V = \sqrt{\frac{2 K_g R T_T}{K - 1} \left\{ 1 - \left(\frac{p}{p_T} \right)^{\frac{K-1}{K}} \right\}} \qquad (1)$$

The total temperature, T_T; static temperature, T; and indicated temperature are related by the experimentally determined recovery factor, λ, which is defined as

$$\lambda = \frac{T_i - T}{T_T - T} \qquad (2)$$

From the assumption of isentropic flow

$$\frac{T}{T_T} = \left(\frac{p}{p_T} \right)^{\frac{K-1}{K}} = r^{\frac{K-1}{K}} \qquad (3)$$

Substitution of Eq 3 for T in Eq 2 obtains

$$T_T = \frac{T_i}{\left(\lambda + (1 - \lambda)\, r^{\frac{K-1}{K}}\right)} \tag{4}$$

Upon substituting Eq 4 in Eq 1,

$$V = \sqrt{\frac{2\,K\,g\,R}{K-1}}\ \sqrt{T_i}\ \sqrt{\frac{1 - r^{\frac{K-1}{K}}}{\left(\lambda + (1 - \lambda)\, r^{\frac{K-1}{K}}\right)}} \tag{5}$$

A further relation for velocity may be obtained by assuming incompressible flow and applying a factor, Y, to correct for the effects of compressibility. Thus

$$V = Y\sqrt{2g\,h_s} = Y\sqrt{\frac{2g}{\gamma}\,(p_T - p_s)} \tag{6}$$

Further assuming $T_i = T$

$$V = Y\sqrt{2gR}\sqrt{T_i}\sqrt{\frac{1 - r}{r}} \tag{7}$$

A relation for this compressibility factor can now be obtained by combining Eqs 5 and 7

$$Y = \frac{V}{\sqrt{2\,g\,R}\sqrt{T_i}\sqrt{\frac{1 - r}{r}}} =$$

$$Y = \sqrt{\frac{K}{K-1}}\sqrt{\frac{r}{1-r}}\sqrt{\frac{\left(1 - r^{\frac{K-1}{K}}\right)}{\left(\lambda + (1 - \lambda)\, r^{\frac{K-1}{K}}\right)}} \tag{8}$$

In a similar manner the mass-rate of flow can be determined.

$$M = \rho V A$$

$$= \frac{p}{gRT} \cdot A \cdot \sqrt{\frac{2 K g R T_T}{K-1} \left(1 - r^{\frac{K-1}{K}}\right)} \qquad (8)$$

$$= \frac{A p}{\sqrt{T_T}} \sqrt{\frac{2K}{gR(K-1)}} \sqrt{\left(r^{\frac{2}{K}} - r^{\frac{K+1}{K}}\right)} \qquad (9)$$

Thus from Eqs 4 and 9,

$$\rho V A = \sqrt{\frac{2K}{gR(K-1)}} \cdot \frac{A p}{\sqrt{T_1}} \cdot \frac{1}{r^{(K-1)/K}} \sqrt{(1-r^{(K-1)/K})\left\{\lambda + (1-\lambda) r^{(K-1)/K}\right\}} \qquad (10)$$

Again assuming incompressible flow and $T = T_1$

$$\rho V A = \frac{Z p A}{g R T_1} \sqrt{2 g h_a} = Z \frac{p A}{g R T_1} \cdot \sqrt{2 g R} \cdot \sqrt{T_1} \sqrt{\frac{1-r}{r}}$$

$$= \frac{Z p A}{\sqrt{T_1}} \sqrt{\frac{2}{gR}} \sqrt{\frac{1-r}{r}} \qquad (11)$$

where Z is a factor to correct for the effects of compressibility.

An expression for Z can be obtained by combining Eqs 10 and 11.

$$Z = \sqrt{\frac{K}{K-1}} \sqrt{\frac{r}{1-r}} \frac{1}{r^{(K-1)/K}} \sqrt{(1 - r^{(K-1)/K})\left(\lambda + (1-\lambda) r^{(K-1)/K}\right)} \qquad (12)$$

The compressibility factor to be used in calculating the kinetic energy was based on the previous two factors, as the following indicates. The weight flow past any section normal to the flow in a time, Δt, is

$\rho V A \Delta t$. Each pound passing in that time has kinetic energy equal to $V^2/2g$. The total kinetic energy passing that section in time, Δt, therefore, is

$$E = \frac{1}{2} (\rho V A) (V^2) \Delta t$$

Substituting for ρVA and V from equations 11 and 7 respectively,

$$E = (Z Y^2) \frac{p A}{T_1} \sqrt{\frac{2g}{R}} (h_a)^{3/2} \Delta t \qquad (13)$$

which may be simplified by introducing the compressibility factor, W, where

$$W = (Z Y^2)$$

Values of Y, Z, and W have been plotted in Figure 17 for recovery factors of 0.8 and 1.0.

Mass-Rate Ratio

The mass-rate ratio was defined as $m = M_x/M_i$. M_x and M_1 can be found from the integral

$$M_x = \int_{A_x} \rho V \cos\phi \, d A \qquad (14)$$

where ϕ is the angle between the velocity vector and a line parallel to the flap. Thus

$$m = \frac{\int_{A_x} \rho V \cos\phi \, d A}{\int_{A_1} \rho V \, d A} \qquad (15)$$

Substituting Eq 11 for ρV.

$$m = \frac{\int_{A_x} \frac{Zp}{T_1} \sqrt{h_a} \cos\phi \; dA}{\left(b\, w \frac{p}{T_1} \sqrt{h_a}\right)_1} \qquad (16)$$

Assuming the specific weight of the fluid at any section to be equal to a mean specific weight calculated from average value of static pressure and temperature,

$$m = \frac{\sqrt{\frac{p}{T_1}} \int_{A_x} Z \sqrt{h_M} \cos\phi \; dA}{\left(\sqrt{\frac{p}{T_1}} \; b\, w\, Z \sqrt{h_m}\right)_1} \qquad (17)$$

Energy Ratio

In a similar manner an expression was obtained for the energy ratio by defining it as $e = E_x / E_1$. Using reasoning similar to that used in deriving Eq 13,

$$e = \frac{\int_{A_x} (\rho V \cos\phi) \cdot V^2 \, dA \, \Delta t}{\int_{A_1} (\rho V) \, V^2 \, dA \, \Delta T} \qquad (18)$$

Substituting for V and ρ V from Eqs 6 and 11 respectively,

$$e = \frac{\int_{A_x} w \cos\phi \, (h_m)^{3/2} \sqrt{\frac{T_1}{p}} \, dA}{\left(b\, w\, w \, (h_m)^{3/2} \sqrt{\frac{T_1}{p}}\right)_1} \qquad (19)$$

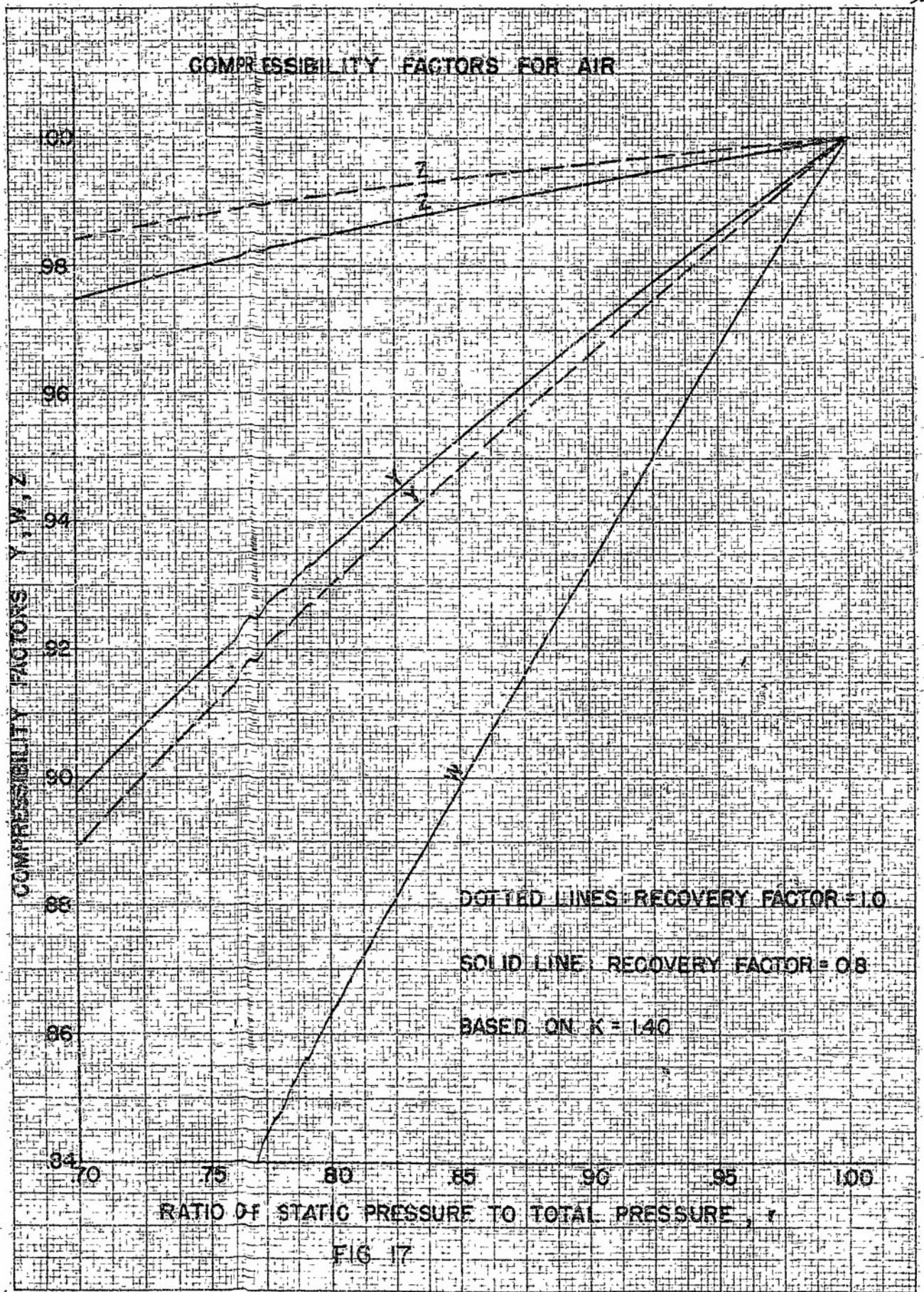
COMPRESSIBILITY FACTORS FOR AIR
100
98
96
94
92
90
88
86
84
70
75
80
85
90
95
100
COMPRESSIBILITY FACTORS Y , W , Z
RATIO OF STATIC PRESSURE TO TOTAL PRESSURE , r
Z
Z
Y
Y
W
DOTTED LINES RECOVERY FACTOR = 1.0
SOLID LINE RECOVERY FACTOR = 0.8
BASED ON K = 1.40

FIG 17

Again assuming the specific weight constant across any one section,

$$e = \frac{\sqrt{\frac{T_1}{p}} \int_{A_x} w \cos\phi \, (h_m)^{3/2} \, dA}{\left(b \, w \, (h_m)^{3/2} \sqrt{\frac{T_1}{p}} \right)_1} \qquad (20)$$